

NON-ITERATIVE NUMERICAL SIMULATION IN VIRTUAL ANALOG: A FRAMEWORK INCORPORATING CURRENT TRENDS

Alessia Andò^{*}, Enrico Bozzo[†] and Federico Fontana[‡]

Department of Mathematics, Computer Science and Physics
University of Udine
Udine, Italy

{alessia.ando, enrico.bozzo, federico.fontana}@uniud.it

ABSTRACT

For their low and constant computational cost, non-iterative methods for the solution of differential problems are gaining popularity in virtual analog provided their stability properties and accuracy level afford their use at no exaggerate temporal oversampling. At least in some application case studies, one recent family of non-iterative schemes has shown promise to outperform methods that achieve accurate results at the cost of iterating several times while converging to the numerical solution. Here, this family is contextualized and studied against known classes of non-iterative methods. The results from these studies foster a more general discussion about the possibilities, role and prospective use of non-iterative methods in virtual analog.

1. INTRODUCTION

Virtual analog provides digital twins of a variety of acoustic systems [1] and electronic circuits [2] responsible of the production and manipulation of sounds. In spite of the niche it occupies among many important application domains of numerical analysis, virtual analog continues to stimulate the development and testing of methods for the solution of ordinary differential equations (ODEs) modeling the problem.

The role of such methods is pivotal. Since they operate between the ODE-based model and its software implementation, any bottleneck caused by an erroneous choice or configuration of the method propagates on the performance of the end product. Compared to other application domains, accuracy is only one factor determining the performances in virtual analog. These applications in fact additionally need to run in real time with no perceivable latency and, more critical, they must respond instantaneously and with realism to model parameter changes even when these are operated abruptly by the performing musician. Accuracy, latency and adaptation to parametric changes at runtime together represent a challenging set of constraints a numerical method must meet for

a virtual analog model to become a digital synthesizer or audio effect at the state of the art. Such constraints are further exacerbated by the limited computational resources available when the virtual analog software runs on dedicated hardware, such as a digital piano or stand-alone audio effect.

While feed-forward signal processing models are straightforwardly mapped in corresponding software procedures [3] that do not need numerical methods for their solution, conversely feedback structures propagating the signal with zero delay must often be computed with the help of a solver when they contain one or more tunable parameters [4] and/or one or more nonlinear maps [5]: in fact, in both cases a structural transformation in a model-equivalent feed-forward structure can be approximate or impossible [6, 7]. After the Newton-Raphson (NR) method was long believed to optimally accommodate virtual analog feedback structures [8, 9, 10, 11], only recently the selection of an optimal iterative solver in Kirchhoff- and Wave-based models has been issued by conducting rigorous formal analyses [12, 13, 14, 15].

Looking at efficiency, *non-iterative* solvers started to be considered by the virtual analog community as a practicable alternative to fixed-point and NR methods: provided they do not drift too far away—perceptually speaking—from the trajectory of the exact solution, the advantage they offer in terms of computation time can counterbalance the higher accuracy an iterative method achieves, yet often at the cost of many iterations. More importantly, non-iterative solvers are supposed to guarantee constancy of the computation time: this feature is especially desirable in virtual analog, where unpredictable changes of the temporal latency at runtime due to varying number of iterations made by, e.g., NR solvers, can affect sound quality much more than numerical inaccuracy as that potentially caused by a non-iterative method.

Among these solvers, a family of methods has been proposed [16, 17] showing attractive characteristics of stability, accuracy and computation time in benchmark case studies limited to uncoupled nonlinearities, such as diode-based clipping and ring modulation. This family is waiting for a systematization and an at least initial performance comparison against the numerous classes of non-iterative numerical methods that have been object of research for decades. For this reason, in Section 2 we pose a differential problem that includes the aforementioned benchmark cases and admits a numerical solution using different classes. After demystifying the non-iterative assumption in Section 3, we classify this family in Section 4. In particular we address exponential methods, a non-iterative class that has not been object of attention in the virtual analog community. Then, in Section 5 stability criteria are recalled that are valid for the classes of interest. Finally, the performances of four solvers belonging to such classes are compared on a diode clipper and ring modulator in Section 6 using param-

^{*} Alessia Andò is a member of *Gruppo Nazionale per il Calcolo Scientifico* (GNCS) of *Istituto Nazionale di Alta Matematica* (INdAM) and is partially supported by the MUR-PRIN 2020 project 2020JLWP23 “Integrated Mathematical Approaches to Socio-Epidemiological Dynamics” (CUP G25F220 00430006).

[†] Enrico Bozzo is a member of *Gruppo Nazionale per il Calcolo Scientifico* (GNCS) of *Istituto Nazionale di Alta Matematica* (INdAM)

[‡] Corresponding Author

Copyright: © 2025 Alessia Andò et al. This is an open-access article distributed under the terms of the Creative Commons Attribution 4.0 International License, which permits unrestricted use, distribution, adaptation, and reproduction in any medium, provided the original author and source are credited.

ters that set both simulations at their stability limit; the results are discussed in Section 7. Section 8 concludes the paper.

The main goal of this work is to set a rigorous framework where the numerical features, stability properties and computational performance of non-iterative methods can be studied in future research.

2. DIFFERENTIAL PROBLEM

Let us consider the following autonomous stiff ODE system involving a vector of signals $x(t)$ and a vector of nonlinear scalar functions $f(x)$ on the same signal

$$\dot{x} + f(x) = 0, \quad (1)$$

whose integral formulation is given by

$$x(t) = x(t_0) - \int_{t_0}^t f(x(u)) du. \quad (2)$$

A numerical approximation of the solution of (1) with $x(t_0) = z_0$ and sampling interval T is defined by a sequence $\{z_n\}_{0 \leq n \leq N}$ such that $z_n \approx x(nT)$. The trapezoidal method is a basic implicit method for its numerical solution having global second order, and taking the form

$$z_{n+1} = z_n - \frac{T}{2}(f(z_n) + f(z_{n+1})). \quad (3)$$

Since the unknown vector z_{n+1} is present in (3) also as an argument of the nonlinearity, a numerical solution must be found. As we said in the introduction, employing iterative methods such as NR for computing the solution usually guarantees sufficient control on the accuracy of the results, provided the existence of favorable convergence properties [13]. At the same time, issues of convergence speed of the iterative process may cause unpredictability of the computation time.

3. TERMINOLOGY

The trapezoidal method, defined by (3), prescribes the value of z_{n+1} —the numerical solution of (1) at time $(n+1)T$ —only implicitly. In other words, z_{n+1} cannot be determined by the simple evaluation of the right-hand side of (3), since the latter depends (non-linearly) in turn on z_{n+1} . All methods sharing the same property are thus termed *implicit* and, as already observed, involve the use of iterative methods. Conversely, *explicit* methods are those which are not implicit, namely those which provide the value of z_{n+1} in terms of a defined sequence of mathematical operations which depend only on z_n, z_{n-1} and so on.

Recent jargon in the virtual analog field calls explicit methods *non-iterative* since they compute the term z_{n+1} without the need of an iterative process. To be more precise, however, while non-iterative methods do not *require* by own definition the use of iterations, iterative processes can still be employed to compute their numerical solution. For instance, certain classes of explicit methods involve the solution of one or more linear systems when applied to non-scalar ODEs. When these systems are small, a direct (i.e., non-iterative) solver such as Gaussian elimination with pivoting can be a valid option. However, for large and sparse linear systems iterative solutions are usually more efficient (see, e.g.,

[18] for an introduction to these algorithms). Thus, these methods might sometimes rely on iterative algorithms for solving linear systems.

In the numerical analysis literature, explicit methods potentially requiring the solution of a sequence of linear systems are sometimes termed *linearly implicit* (or *semi-implicit*). This is because the sequence of linear systems is meant to replace the non-linear solution occurring in implicit methods, and thus to avoid the *necessity* to resort to iterative methods. In the following we will adhere to the terminology specified by this literature.

4. SIMULATION METHODS

We consider four classes of non-iterative methods, whose mutual relationships will be clarified at the end of the section.

4.1. Rosenbrock and Rosenbrock-Wanner methods

The fundamental idea introduced by Rosenbrock [19], already adopted in virtual analog [20], is to perform just one step of the NR method starting from z_n in order to avoid issues of convergence of the iterative process. This procedure defines the following linearly implicit scheme (for multidimensional systems the fraction and division operators have to be interpreted as a multiplication by the inverse appearing at the denominator)

$$z_{n+1} = z_n - \frac{Tf(z_n)}{1 + \frac{T}{2}f'(z_n)}, \quad (4)$$

again global second order, which belongs to the broader family of Rosenbrock methods. Indeed, he used this idea to build higher order multistage methods, and after his seminal paper a lot of work has been done around his proposal (a review can be found in [21]). In particular, developments include the family of linearly implicit Rosenbrock-Wanner (ROW) methods [22], which only use the Jacobian $f'(z_n)$ for the entire $(n+1)$ -th step, regardless of the number of stages, and have strong stability properties. Their general form is

$$\begin{aligned} & (I + T\gamma_{ii}f'(z_n))K_i \\ &= -Tf\left(z_n + \sum_{j=1}^{i-1} \alpha_{ij}K_j\right) - Tf'(z_n) \sum_{j=1}^{i-1} \gamma_{ij}K_j, \\ & i = 1, \dots, s, \\ & z_{n+1} = z_n + \sum_{i=1}^s b_i K_i. \end{aligned} \quad (5)$$

Notice that (4) is obtained when $s = 1$, $b_1 = 1$ and $\gamma_{11} = 1/2$. An interesting example of a ROW method is implemented by the `ode23s` MATLAB function. The implementation involves two schemes having two and three stages, respectively. The comparison of the result obtained with both schemes at each temporal step provides an estimate of the error, which is then used to adapt the time step-size. Using the results in [23], the method can be reformulated so as to minimize the number of matrix multiplications,

as follows:

$$\begin{aligned}
 (I + Tdf'(z_n))K_1 &= -Tf(z_n) \\
 (I + Tdf'(z_n))K_2 &= -Tf\left(z_n + \frac{1}{2}K_1\right) - Tdf'(z_n)K_1 \\
 z_{n+1} &= z_n + K_2, \\
 (I + Tdf'(z_n))K_3 &= -Tf(z_{n+1}) - e\left(K_2 + Tf\left(z_n + \frac{1}{2}K_1\right)\right) \\
 &\quad - 2(K_1 + Tf(z_n)) \\
 \text{err} &\approx \frac{K_1 - 2K_2 + K_3}{6},
 \end{aligned} \tag{6}$$

where $d = \frac{1}{2+\sqrt{2}}$ and $e = 6 + \sqrt{2}$.

4.2. Rational approximation methods

By “rational approximation methods” we refer to single-stage methods whose idea is to approximate higher-order derivatives of the numerical solution of (1) in terms of f and its derivatives. For instance, one has

$$\begin{aligned}
 z'_n &\approx -f(z_n) \\
 z''_n &\approx f'(z_n)f(z_n) \\
 z'''_n &\approx -f(z_n)(f''(z_n)f(z_n) + f'(z_n)f'(z_n))
 \end{aligned}$$

and so on. The general expression of a rational approximation method has the form

$$z_{n+1} = z_n + \frac{p_M(T)}{q_N(T)}, \tag{7}$$

where the polynomials p_M and q_N have degrees M and N respectively, and their coefficients are in turn multivariate polynomials in the derivatives of f at z_n .

In [17], but see also [16], the authors present a family of rational schemes suitable for the numerical solution of stiff ODEs arising in virtual analog modeling. Each scheme of the family is characterized by an index $P = 0, 1, 2, \dots$ and takes the form

$$\sigma^{(P)}(z_n) \frac{z_{n+1} - z_n}{T} + g(z_n) \frac{z_{n+1} + z_n}{2} = 0, \tag{8}$$

where $g(x) = f(x)/x$. As noted in [24], the presence of the ratio $f(x)/x$ causes a severe restriction on the applicability of the scheme to multidimensional systems. Solving with respect to z_{n+1} yields

$$z_{n+1} = z_n - \frac{Tz_ng(z_n)}{\sigma^{(P)}(z_n) + \frac{T}{2}g(z_n)} = z_n - \frac{Tf(z_n)}{\sigma^{(P)}(z_n) + \frac{T}{2}g(z_n)} \tag{9}$$

The scheme of index P has global order $P+1$ and involves derivatives of f up to order P . According to [16], when $P = 1$ the method becomes especially suitable for the simulation of audio circuits. In this case

$$\sigma^{(1)}(x) = 1 + \frac{T}{2}(f'(x) - g(x)), \tag{10}$$

and substituting in (9) yields (4). Hence, (8) when $P = 1$ is the first method (4) proposed by Rosenbrock. When $P = 2$,

$$\sigma^2(x) = 1 + \frac{T}{2}(f'(x) - g(x)) + \frac{T^2}{12}((f'(x))^2 - 2f(x)f''(x)),$$

and substituting in (9) leads to the scheme

$$z_{n+1} = z_n - \frac{Tf(z_n)}{1 + \frac{T}{2}f'(z_n) + \frac{T^2}{12}((f'(z_n))^2 - 2f(z_n)f''(z_n))}, \tag{11}$$

an expression showing that the scheme belongs to the family (7) of rational approximation methods.

4.3. Exponential methods

Exponential methods define a non-iterative class that was specifically developed to overcome the problem of stiffness [25]. They are employed to solve semi-linear problems of the form

$$\dot{x}(t) = f(t, x(t)) = Lx(t) + N(t, x(t)), \tag{12}$$

where L is a linear term which approximates the Jacobian of f . This translates into requiring that the nonlinear term N is non- or only mildly stiff. Exponential methods integrate the linear part L exactly, so that its stiffness properties do not constitute an issue.

The subclass of exponential time-differencing (ETD) methods are based on the use of the *variation of constant formula*, which can also be obtained by observing that, from (12),

$$\frac{d(e^{-Lt}x(t))}{dt} = e^{-Lt}N(t, x(t)).$$

Indeed, integrating the latter from $t = t_n$ to $t_{n+1} = t_n + h$ gives

$$x(t_{n+1}) = e^{hL}x(t_n) + e^{hL} \int_0^h e^{(t-s)L}N(t_n + s, x(t_n + s))ds.$$

The variation of constants formula above is exact, and what characterizes a specific ETD method is the way the nonlinear term in the integral is approximated. The simplest possible approximation is defined by the constant $N_n := N(t_n, x(t_n))$, which gives the Nørsett-Euler method, first derived in [26]:

$$z_{n+1} = e^{hL}z_n + \frac{e^{hL} - I}{L}N_n. \tag{13}$$

Research on ETD methods has not abated (see [27] for a general review on exponential methods) and methods converging with order up to 6 have been derived [28]. ETD methods are closely related to W-methods [29], which in turn were developed from the class of Rosenbrock methods with the idea of avoiding the computation of exact Jacobians at every time step. W-methods do not belong to the ETD subclass, however they can be seen as an approximation of ETD methods, where the exponential and related matrix functions are not computed exactly, but rather via Padé approximations.

For ODEs which cannot be formulated as (12) (that is, no constant approximation L of the Jacobian is available), an alternative is to compute them using exponential Rosenbrock methods. To explain the idea behind them, for the sake of simplicity of the notation, we consider autonomous ODEs of the form $\dot{x}(t) = f(x(t))$. Exponential Rosenbrock methods treat the ODE as semi-linear, with (varying) linear part $L_n = \frac{\partial f}{\partial x}(z_n)$ and $N_n(x(t)) =$

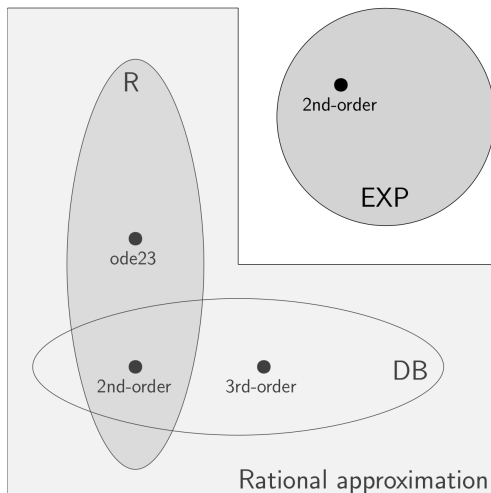


Figure 1: Set relationships among considered methods. *R*: Rosenbrock type; *DB*: Ducceschi-Bilbao; *EXP*: exponential. Dotted elements correspond to schemes studied in this paper.

$f(x(t)) - L_n x(t)$. In particular, the exponential Rosenbrock-Euler method is defined by (13) with L being replaced by L_n :

$$z_{n+1} = e^{hL_n} z_n + \frac{e^{hL_n} - I}{L_n} N_n. \quad (14)$$

4.4. Relationships among the proposed methods

In conclusion, the proposed methods define three classes as in Fig. 1. From here on we will label two-stage Rosenbrock (6), second-order Rosenbrock (10) [17], third-order Ducceschi-Bilbao (11) [16] and exponential (14) respectively as ODE23, DB I, DB II, and EXP.

5. A- AND L-STABILITY

Let us reconsider (1) in which $f(x) = -\lambda x$ and $x(t_0) = 1$ where, for generality, $\lambda \in \mathbb{C}$. This is known as the *test* equation. All schemes introduced so far, when applied to the test equation, yield a recurrence of the form $z_{n+1} = R(w)z_n$, where $w = \lambda T$. For example, for the scheme (4) it is not difficult to check that

$$R(w) = \frac{2+w}{2-w}. \quad (15)$$

The function R is known as stability function of the method; the set $S = \{w \in \mathbb{C} : |R(w)| < 1\}$ is its stability domain. A scheme is called *A*-stable if the negative half of the complex plane is contained in S . For example, the scheme (4) is *A*-stable since

$$|R(w)|^2 = \frac{\alpha^2 + \beta^2 + 4 + 2\alpha}{\alpha^2 + \beta^2 + 4 - 2\alpha},$$

where $\alpha = \Re(w)$ and $\beta = \Im(w)$, and obviously

$$\alpha^2 + \beta^2 + 4 - 2\alpha > \alpha^2 + \beta^2 + 4 + 2\alpha \Leftrightarrow \alpha < 0.$$

Besides (4), the schemes (6), (14) and (11) are all *A*-stable. An important result, known as the Dahlquist barrier [30], states that there does not exist a *A*-stable method whose order is larger than 2

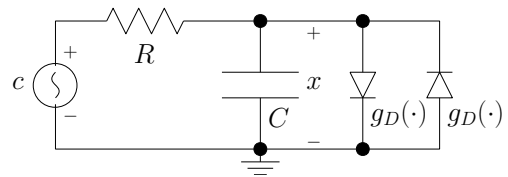


Figure 2: Diode clipper: electronic circuit.

in the class of constant coefficients linear multistep (LMS) methods. For example, the trapezoidal method is an LMS method of the largest possible order. Of course, the method (11) is rational, but not LMS. In turn, (4), (6) and (14) are not LMS methods.

If a method is *A*-stable and in addition $\lim_{w \rightarrow -\infty} R(w) = 0$, then it is defined *L*-stable. An *L*-stable method works well for those w with a large negative real part. Since

$$\lim_{w \rightarrow -\infty} \frac{2+w}{2-w} = -1,$$

the scheme (4) is not *L*-stable. Of the discussed schemes only (6) is *L*-stable: its parameters d and e are set to guarantee this property.

Although *A*- and *L*-stability are generally desirable (and often considered to be necessary) properties, they cannot predict precisely the behavior of a method on a specific initial-value problem. This is particularly evident if the function f in (1) contains strong nonlinearities, since the stability function restricts the test to linear equations.

6. CASE STUDIES

Four simulations, running ODE23, DB I, DB II, and EXP, are compared in this section on two different analog effects using circuit parameters as those adopted in [16, 17].

6.1. Diode clipper

The diode clipper in Fig. 2 is traditionally used as a test bed in several virtual analog publications [20]. The two diodes form a circuit nonlinearity, whose stiffness properties were formally analyzed [11]. In particular, convergence in NR-based simulations of this system has been shown to slow down, becoming potentially critical when the resistance of either diode rapidly increases against a negative applied voltage provided by the capacitor, in its turn fed by the input signal $c(t)$ [13].

Fig. 3 (top) plots the case where a $8 \cdot 48$ kHz sampling rate is set, with a 16 V sinusoid at 2 kHz as input for all four simulations. It can be observed that, due to the relatively high voltage, this input creates some artifacts in correspondence of the aforementioned critical working point of the diode which are largest for EXP. At this input voltage the system is close to instability: for instance, a 17 V sinusoid at 2 kHz, see Fig. 3 (bottom), causes an unrecoverable drift of DB II however in presence of a more accurate behavior of EXP; if set at 19 V, the same sinusoid provokes a numerical explosion of the ODE23-based simulator (not displayed in the figure).

6.2. Ring modulator

Thanks to a circuit loop connecting four identical diodes, the ring modulator shown in Fig. 4 generates an output representing the

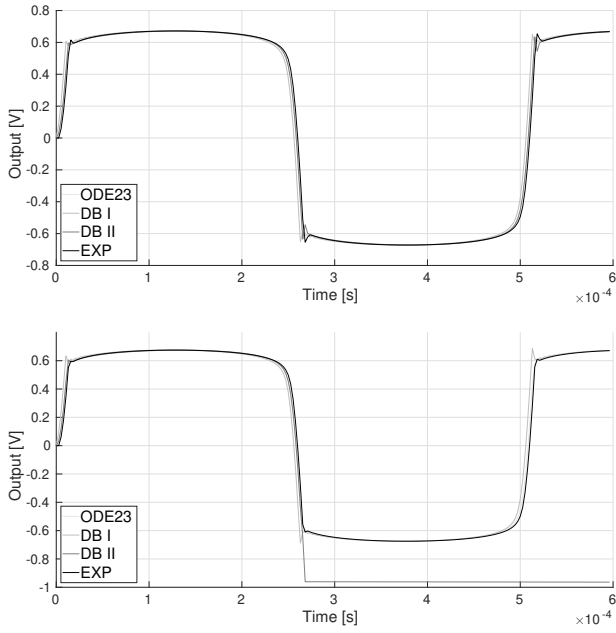


Figure 3: Diode clipper: output signals from ODE23, DB I, DB II, EXP simulations with a 16 V (top) and 17 V (bottom) input sinusoid $c(t)$ at 2 kHz; sampling rate set to $8 \cdot 48$ kHz.

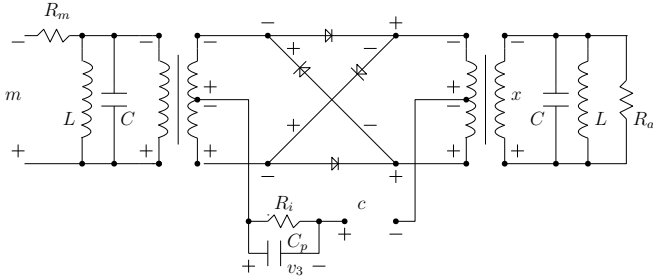


Figure 4: Ring modulator: electronic circuit.

product of two inputs, a modulator $m(t)$ and a carrier voltage signal $c(t)$ [31]. Also in this case, it has been shown that NR-based simulators need a longer iterative process when the analog product of the inputs becomes large, also depending on the magnitude of the carrier signal, hence they critically slow down proportionally to the output signal magnitude when the carrier signal is comparable [13].

Fig. 5 (top) plots the case when a $8 \cdot 48$ kHz sampling rate is set, with a 1.2 V modulating sinusoid at 4 kHz carried by a 0.7 V sinusoid oscillating at 4 kHz for all four simulations. It can be observed that some small artifacts arise when using DB II in correspondence of a point (at about 0.4 ms) where the computational effort is highest. Also in this case, with these input parameters the system is close to instability: increasing the amplitude of the carrier sinusoid to 0.8 V, see Fig. 5 (bottom), again causes an unrecoverable deviation of DB II yet with no loss of accuracy of the other methods.

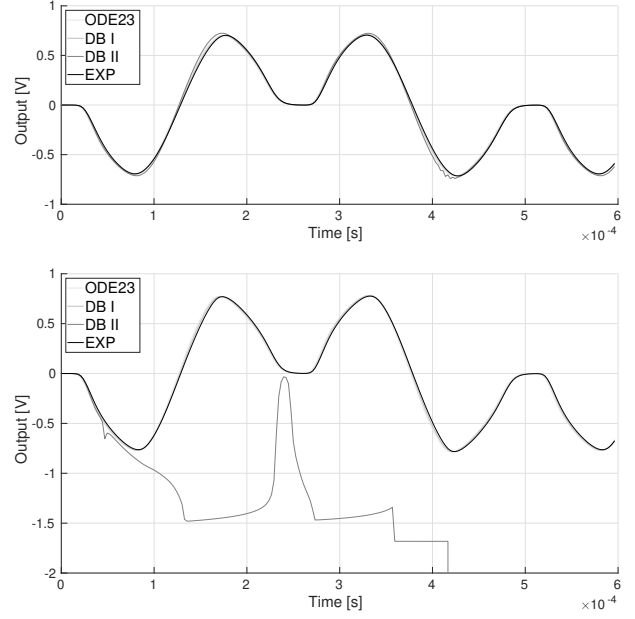


Figure 5: Ring modulator: output signals from ODE23, DB I, DB II, EXP simulations with a 0.7 V (top) and 0.8 V (bottom) input carrier sinusoid $c(t)$ at 8 kHz along with a 1.2 V input modulating sinusoid $m(t)$ at 4 kHz; sampling rate set to $8 \cdot 48$ kHz.

7. DISCUSSION

A comparison of the four methods performed on a Linux laptop mounting twelve Intel(R) Core(TM) i7-10710U CPU @ 1.10GHz, running Matlab 2024b in both studies, leads to the relative computation times in Table 1 specifically referring to the stable simulations shown in Fig. 3 (top) and 5 (top). All such simulations are ways faster than those based on NR, as ascertained by previous literature [17]. Thanks to A- and L-stability, all methods are able

Table 1: Case studies: Relative computation times with oversampling factor set to $8 \cdot 48$ kHz, leading to the plots in Figs. 6 and 7 (top). Unitary relative computation time corresponds to 0.25 s (diode clipper) and 0.16 s (ring modulator) respectively for a 12 s and 1 s simulation.

	ODE23	DB I	DB II	EXP
Diode clipper	1.74	1.00	1.10	1.23
Ring modulator	2.19	1.00	2.06	6.17

to simulate critical behaviors that have been induced by injecting especially high input voltages.

An inspection of the corresponding magnitude spectra, above in Figs. 6 and 7 for the diode clipper and the ring modulator respectively, shows high similarity in the audio band using the adopted oversampling factor, yet with magnitude differences of the peak components generated by DB I and especially DB II increasing with frequency. Such differences produce peaks having approximately twice as many dB near the Nyquist frequency in the diode clipper simulation; in parallel, they result in an oscillatory drift caused by DB II when simulating the ring modulator. In the case of DB II these drifts are explained by the inaccurate computation of

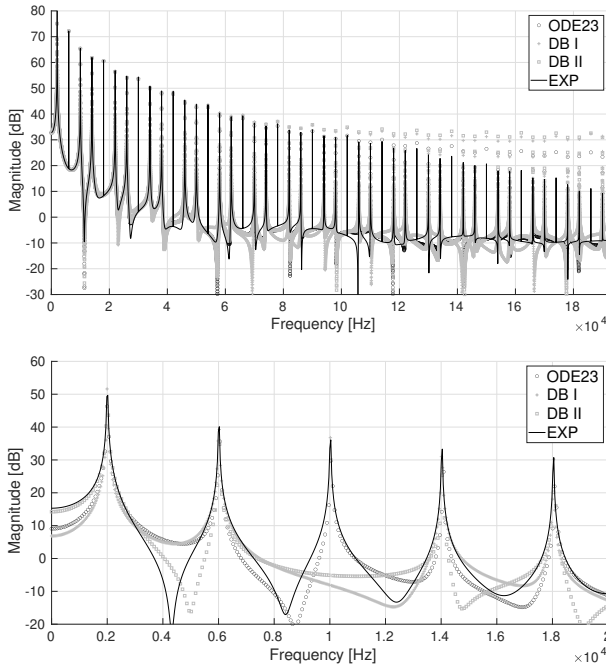


Figure 6: Diode clipper: magnitude spectra from ODE23, DB I, DB II, EXP simulations with an 8 V input sinusoid $c(t)$ at 2 kHz; sampling rate set to $8 \cdot 48$ kHz (top) or to values resulting in peak magnitude differences smaller than approximately 6 dB in the $[0, 20]$ kHz frequency range (bottom).

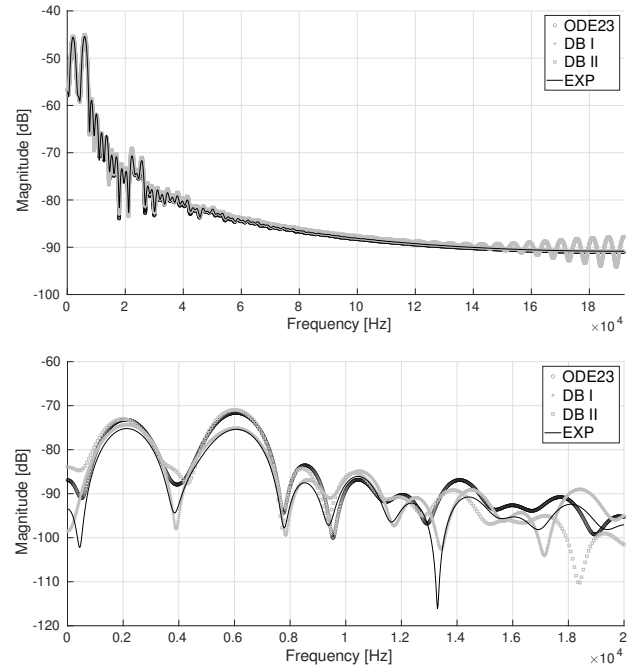


Figure 7: Ring modulator: magnitude spectra from ODE23, DB I, DB II, EXP simulations with a 0.35 V input carrier sinusoid $c(t)$ at 8 kHz along with a 1.2 V input modulating sinusoid $m(t)$ at 4 kHz; sampling rate set to $8 \cdot 48$ kHz (top) or to values resulting in peak magnitude differences smaller than approximately 6 dB in the $[0, 20]$ kHz frequency range (bottom).

the denominator in (11), negatively conditioning the corresponding matrix inversion problem that becomes necessary in the multi-dimensional case.

Overall, the observed spectral differences suggest a variable numerical behavior of the four methods. We inspect in particular the audio frequency band, by respectively selecting oversampling factors capable of equalizing the spectral peaks resulting by each method within an overall tolerance equal to approximately 6 dB up to 20 kHz. The results are plotted below in Figs. 6 and 7, respectively for the diode clipper and the ring modulator. In both systems, we set the corresponding critical input $c(t)$ to half the amplitude keeping them close to instability, that is, 8 V instead of 16 V for the diode clipper and 0.35 V instead of 0.7 V for the ring modulator. In this way, a sufficient range is created in which to set the oversampling factor.

Table 2: Case studies: relative computation times and factors oversampling 48 kHz leading to the plots in Figs. 6 and 7 (bottom). Best performance in bold characters.

	ODE23	DB I	DB II	EXP
Diode clipper: time	2.84	1.00	2.23	1.01
oversampling factor	5.83	3.33	6.66	2.92
Ring modulator: time	2.41	1.00	2.03	13.56
oversampling factor	1.17	1.00	5.42	1.67

Table 2 summarizes the performance of the methods we tested on both systems. Concerning the diode clipper, DB I and then

EXP perform the best, with the longer time to compute one output value in EXP being compensated by the smaller oversampling factor; conversely, ODE23 performs the worst despite the smaller oversampling factor that can be set compared to DB II. In the ring modulator case, DB I wins in terms of both computation time and oversampling factor, whereas EXP slips to the last position despite a fair oversampling factor, meaning that the time to compute the matrix exponentials in (13) becomes too long; DB II and ODE23 both show acceptable performances, even if the former requires the largest oversampling factor in this case also.

8. CONCLUSIONS

In spite of its limited scope, our investigation on four methods that do not explicitly expose an iterative solution—such as NR does—speaks in favor of a significant dependence of their numerical performances on the ODEs that need to be integrated. Among such methods, second-order Rosenbrock seems to be the best choice as long as the size of the differential problem is compact, as previously suggested [17]. Exponential-Rosenbrock methods can also be used for the numerical solution of oscillatory [32] systems; these systems find application for modeling, among others, switching problems in musical acoustics—see e.g. [33]. In parallel, Port-Hamiltonian systems have already proved to provide explicit second-order passive guaranteed solutions [34, 35, 36]. More in general, passivity plays a key role for realizing stable virtual analog systems thanks to theoretical tools such as the Lya-

punov theory of discrete state-space systems [37].

The literature on non-iterative methods is certainly not restricted to those we examined here, and various recent works suggest that the topic is still lively. For example, in [38] a parametric family has been proposed allowing the selection of a global second-order A -stable method originally proposed in [39]. Moreover, a careful analysis of the parametric family allows the authors to determine a new L -stable scheme of global second order. In [40] four mixed Rosenbrock-exponential schemes are proposed for problems in the form $\dot{x} = f_1(x) + f_2(x)$, where f_1 and f_2 are nonlinear. These schemes become convenient if either nonlinear function has a Jacobian J such that the linear system whose matrix is $I - TJ$ can be efficiently solved. Similarly, a recently proposed family of methods exploits the idea of multiplying f by an operator known as Time-Accurate highly-Stable Explicit (TASE) operator [41]. As a simple example, applying implicit Euler to the test equation (see Section 5) yields the recurrence $z_{n+1} = z_n/(1 - T\lambda)$; the same recurrence results by applying explicit Euler to the equation $\dot{x} - (1 - T\lambda)^{-1}\lambda x$. Here, $(1 - T\lambda)^{-1} = (1 + TJ)^{-1}$ is the TASE operator. Explicit Runge-Kutta methods are normally chosen among possible candidates to solve the modified equation, requiring the computation of a certain number of linear systems at every step. These methods show excellent stability, and to the best of our knowledge, they have not yet been investigated in the virtual analog field.

9. ACKNOWLEDGMENTS

This work has been partially supported by the MUR-PRIN 2022 project 20229P2HEA “Stochastic numerical modelling for sustainable innovation”.

10. REFERENCES

- [1] N. H. Fletcher and T. D. Rossing, *The Physics of Musical Instruments*, Springer-Verlag, New York, 1991.
- [2] M. Jenkins, *Analog Synthesizers*, Focal Press, 2007.
- [3] S. K. Mitra and J. F. Kaiser, Eds., *Handbook for Digital Signal Processing*, J. Wiley & Sons, New York, NY, USA, 1993.
- [4] F. Fontana, “Preserving the structure of the Moog VCF in the digital domain,” in *Proc. Int. Computer Music Conf.*, Copenhagen, Denmark, 27–31 Aug. 2007, pp. 291–294.
- [5] V. Zavalishin, “The art of VA filter design,” Web available at https://www.discodsp.net/VAFilterDesign_2.1.0.pdf, oct 2018, v. 2.1.0.
- [6] F. Fontana and F. Avanzini, “Computation of delay-free nonlinear digital filter networks. Application to chaotic circuits and intracellular signal transduction,” *IEEE Trans. on Signal Processing*, vol. 56, no. 10, pp. 4703–4715, Oct. 2008.
- [7] D. T. Yeh, J. S. Abel, and J. O. Smith, “Automated physical modeling of nonlinear audio circuits for real-time audio effects – Part I: Theoretical development,” *IEEE Trans. on Audio, Speech and Language Processing*, vol. 18, no. 4, pp. 728–737, 2010.
- [8] W. Ross Dunkel, Maximilian Rest, Kurt James Werner, Michael Jørgen Olsen, and Julius O. Smith, “The Fender Bassman 5F6 - a family of preamplifier circuits - A wave digital filter case study,” in *Proc. 19 Conf. on Digital Audio Effects (DAFx-16)*, Brno, Czech Republic, Sep. 5–9 2016, DAFx, pp. 263–270.
- [9] M. Holters and U. Zölzer, “Automatic decomposition of nonlinear equation systems in audio effect circuit simulation,” in *Proc. 20 Conf. on Digital Audio Effects (DAFx-17)*, Edinburgh, UK, Sep. 5–9 2017, pp. 138–144.
- [10] Jamie Bridges and Maarten van Walstijn, “Modal based tanpura simulation: Combining tension modulation and distributed bridge interaction,” in *Proc. 20 Conf. on Digital Audio Effects (DAFx-17)*, Edinburgh, UK, Sep. 5–9 2017, pp. 299–306.
- [11] Rémy Muller and Thomas Hélie, “Power-balanced modelling of circuits as skew gradient systems,” in *Proc. 21 Conf. on Digital Audio Effects (DAFx-18)*, Aveiro, Portugal, Sep. 4–8 2018, pp. 264–271.
- [12] F. Fontana and E. Bozzo, “Explicit fixed-point computation of nonlinear delay-free loop filter networks,” *IEEE/ACM Trans. on Audio, Speech and Language Processing*, vol. 26, no. 10, pp. 1884–1896, Oct. 2018.
- [13] F. Fontana and E. Bozzo, “Newton-Raphson solution of nonlinear delay-free loop filter networks,” *IEEE/ACM Trans. on Audio, Speech and Language Processing*, vol. 27, no. 10, pp. 1590–1600, Oct. 2019.
- [14] Alberto Bernardini, Enrico Bozzo, Federico Fontana, and Augusto Sarti, “A wave digital Newton-Raphson method for virtual analog modeling of audio circuits with multiple one-port nonlinearities,” *IEEE/ACM Trans. on Audio, Speech and Language Processing*, vol. 29, pp. 2162–2173, 2021.
- [15] Federico Fontana, Enrico Bozzo, and Alberto Bernardini, “Extended fixed-point methods for the computation of virtual analog models,” *IEEE Signal Processing Letters*, vol. 30, pp. 848–852, 2023.
- [16] M. Ducceschi, S. Bilbao, and C. J. Webb, “Non-iterative schemes for the simulation of nonlinear audio circuits,” in *Proc. 24 Conf. on Digital Audio Effects (DAFx20in21)*, Vienna, Austria, Sep. 8–10 2021, pp. 25–32.
- [17] M. Ducceschi and S. Bilbao, “Non-iterative simulation methods for virtual analog modelling,” *IEEE/ACM Trans. on Audio, Speech and Language Processing*, vol. 30, pp. 3189–3198, 2022.
- [18] A. Greenbaum, *Iterative methods for solving linear systems*, Frontiers in Applied Mathematics. SIAM, Philadelphia, 1997.
- [19] H. H. Rosenbrock, “Some general implicit processes for the numerical solution of differential equations,” *The Computer Journal*, vol. 5, pp. 329–330, 1963.
- [20] David T. Yeh, Jonathan Abel, and Julius O Smith, “Simulation of the diode limiter in guitar distortion circuits by numerical solution of ordinary differential equations,” in *Proc. 10 Conf. on Digital Audio Effects (DAFx-07)*, Bordeaux, France, Sep. 10–15 2007, pp. 197–204.
- [21] J. Lang, “Rosenbrock-Wanner methods: construction and mission,” in *Rosenbrock-Wanner-Type Methods*, T. Jax, A. Bartel, M. Ehrhart, M. Günther, and G. Steinebach, Eds., chapter 1, pp. 1–17. Springer, Cham, 2021.

- [22] G. Wanner, “On the integration of stiff differential equations,” in *Numerical Analysis: Proceedings of the Colloquium on Numerical Analysis Lausanne, October 11–13, 1976*, Jean Descloux and Jürg Marti, Eds., pp. 209–226. Birkhäuser Basel, Basel, 1977.
- [23] L. F. Shampine, “Implementation of Rosenbrock methods,” *ACM Trans. Math. Softw.*, vol. 8, no. 2, pp. 93–113, June 1982.
- [24] M. Holters, “Revisiting the second-order accurate non-iterative discretization scheme,” in *Proc. 27 Conf. on Digital Audio Effects (DAFx-24)*, Guildford, UK, Sep. 2-5 2024, pp. 105–110.
- [25] J. Certaine, *The solution of ordinary differential equations with large time constants*, pp. 128–132, Wiley, New York, 1960.
- [26] S. P. Nørsett, “An A-stable modification of Adams-Bashforth’s method for he numerical integration of ordinary stiff differential equations,” *Preprint series: Pure mathematics* <http://urn.nb.no/URN:NBN:no-8076>, 1969.
- [27] M. Hochbruck and A. Ostermann, “Exponential integrators,” *Acta Numerica*, vol. 19, pp. 209–286, 2010.
- [28] V. T. Luan and A. Ostermann, “Parallel exponential Rosenbrock methods,” *Computers & Mathematics with Applications*, vol. 71, no. 5, pp. 1137–1150, 2016.
- [29] T. Steihaug and A. Wolfbrandt, “An attempt to avoid exact jacobian and nonlinear equations in the numerical solution of stiff differential equations,” *Mathematics of Computation*, vol. 33, no. 146, pp. 521–534, 1979.
- [30] D. Givoli, “Dahlquist’s barriers and much beyond,” *Journal of Computational Physics*, vol. 475, pp. 111836, 2023.
- [31] R. Hoffmann-Burchardi, “Digital simulation of the diode ring modulator for musical applications,” in *Proc. 11 Conf. on Digital Audio Effects (DAFx-08)*, Espoo, Finland, Sep. 2008, pp. 165–168.
- [32] Dongfang Li and Xiaoxi Li, “Relaxation exponential rosenbrock-type methods for oscillatory hamiltonian systems,” *SIAM Journal on Scientific Computing*, vol. 45, no. 6, pp. 2886–2911, 2023.
- [33] M. Ducceschi, S. Bilbao, S. Willemsen, and S. Serafin, “Linearly-implicit schemes for collisions in musical acoustics based on energy quadratisation,” *J. of the Acoustical Society of America*, vol. 149, no. 5, May 2021.
- [34] N. Lopes, T. Hélie, and A. Falaize, “Explicit second-order accurate method for the passive guaranteed simulation of port-hamiltonian systems,” *IFAC-PapersOnLine*, vol. 48, no. 13, pp. 223–228, 2015, 5th IFAC Workshop on Lagrangian and Hamiltonian Methods for Nonlinear Control LHMNC 2015.
- [35] Rémy Muller and Thomas Hélie, “Trajectory anti-aliasing on guaranteed-passive simulation of nonlinear physical systems,” in *Proc. 20 Conf. on Digital Audio Effects (DAFx-17)*, Edinmburgh, UK, Sep. 5–9 2017, pp. 87–94.
- [36] M. Danish, S. Bilbao, and M. Ducceschi, “Applications of port hamiltonian methods to non-iterative stable simulations of the korg35 and moog 4-pole vcf,” in *Proc. 24 Conf. on Digital Audio Effects (DAFx20in21)*, Vienna, Austria, Sep. 8–10 2021, pp. 33–40.
- [37] Nicoletta Bof, Ruggero Carli, and Luca Schenato, “Lypunov theory for discrete time systems,” *arXiv preprint arXiv:1809.05289*, 2018.
- [38] H. Ramos, G. Singh, V. Kanwar, and S. Bhatia, “An embedded 3(2) pair of nonlinear methods for solving first order initial-value ordinary differential systems,” *Numerical Algorithms*, vol. 75, pp. 509–529, 2017.
- [39] C. Brezinsky, “Intégration des systèmes différentiels à l’aide du ρ -algorithme,” *Comptes rendus de l’Académie des sciences*, vol. 278 A, pp. 875–878, 1974.
- [40] V. Dallerit, T. Buvoli, M. Tokman, and S. Gaudreault, “Second-order Rosenbrock-exponential (ROSEXP) methods for partitioned differential equations,” *Numerical Algorithms*, vol. 96, pp. 1143–1161, 2024.
- [41] D. Conte, G. Pagano, and B. Paternoster, “Time-accurate and highly-stable explicit peer methods for stiff differential problems,” *Communications in Nonlinear Science and Numerical Simulation*, vol. 119, pp. 107136, 2023.